Design, Synthesis, Characterization, and Modeling of a Series of *S*,*S*-Dioxothienylenevinylene-Based Conjugated Polymers with Evolving Frontier Orbitals

Cheng Zhang,[†] Thuong H. Nguyen,[†] Jianyuan Sun,[†] Rui Li,[†] Suely Black,[†,‡] Carl E. Bonner,[†,‡] and Sam-Shajing Sun*[,†,‡]

Center for Material Research and Chemistry Department, Norfolk State University 700 Park Avenue, Norfolk, Virginia 23504

Received November 21, 2008; Revised Manuscript Received December 10, 2008

ABSTRACT: A series of evolving frontier energy levels and gaps sulfone-containing thienylenevinylene-based conjugated copolymers have been synthesized via the Horner−Emmons reactions between 2,5-bisdiethoxyphosphorylmethyl-3,4-dihexyl-1,1-dioxothiophene and a series of different donor type dialdehyde comonomers. The resulting polymers (SF-PTVs) contain alternating donor (benzene or thiophene ring with/without alkoxy substituents) and acceptor (1,1-dioxothiophene) units. A range of HOMO/LUMO levels and energy gaps (between 1.0 and 2.0 eV) were achieved in these new polymers. The use of oxidized thiophene moiety brings about 0.3 eV in reduction of energy gap. Computational study on the model oligomers of P(C6OTV-SFTV) and related structures reveals that the reduction is mainly due to the removal of aromaticity of the thiophene. The donor−acceptor interaction is also responsible for about one-third or less of the energy gap reduction. Theses polymers have very good thermal stability (dynamically, 258 °C or higher), and their decomposition starts with loss of mass as in contrast to regular PTVs which decompose initially by cross-linking.

1. Introduction

Availability of stable, processable, functionalizable, and evolving low energy gap (E_g) n-type conjugated polymers is critical for developing various types of donor−acceptor (D/A)-based polymer electronic and optoelectronic (OE) devices,[1,2] for instance, devices made of all-polymer D/A bulk heterojunctions[1−3] and donor−acceptor block copolymers.[4] The latter has been the focus of our studies.[5,6] One of the great challenges in D−A block copolymer OE device development is to develop a series of acceptor polymer blocks having the following features: (1) The absorption spectrum covers a good portion of visible solar spectrum (with energy gaps E_g in the range of 1−2 eV). (2) The LUMO level is sufficiently low to enable photoinduced electron transfer from donor polymers and to maintain air stability. (3) End-group functionalities allow covalent coupling with other donor block(s). In general, energy gaps of conjugated polymers may be reduced by incorporating the following structural features: aromatic units with low resonance energy, strongly coupled donor−acceptor substituents, large and coplanar π-systems, high regioregularity of side chains, etc.[7] Because of its low resonance energy and good chemical stability, the thiophene ring has been widely used for developing low energy gap conjugated polymers. Insertion of a C═C bond between every two thiophene rings leads to polythienylenevinylenes (PTVs) with lower E_gs in the range of 1.5−1.8 eV.[8−11] Our goal is to develop new PTV-like polymers having not only low E_gs but also low LUMO levels. A series of novel sulfone (SF)-containing polythienylenetetravinylene repeating unit [P(C6OTV-SFTV) in Scheme 1] has thus been designed and developed. These new polymers can be considered as a PTV with the sulfur in every other thiophene ring being oxidized to sulfone ($-SO_2-$). Oxidation of the sulfur not only causes the thiophene ring to lose its aromaticity but also inserts a strong electron-withdrawing group in the π-conjugated main chain.[12] Significant reductions in both E_g and LUMO levels have been achieved. By using comonomers with different aromatic resonance energy and with/without electron donating side groups, a series of sulfone-containing conjugated polymers with a wide range of energy gaps have been obtained. Furthermore, the terminal functional groups and chemical schemes of these polymers would enable block copolymer supramolecular structure developments.

2. Experimental Section

Starting Materials and Instrumentation. All starting materials, reagents, and solvents were purchased from commercial sources (Sigma Aldrich and Fisher-Scientific) and used as received unless noted otherwise. NMR spectra were obtained from a Bruker Advance 300 MHz spectrometer with TMS as the internal reference. Elemental analysis was performed by Atlantic Microlab Inc. UV−vis data were collected on a Perkin-Elmer Lambda 900 spectrophotometer. Photoluminescence experiments were performed on an ISA Fluoromax-3 luminescence spectrofluorometer. Differential scanning calorimeter (DSC) and thermal gravimetric analyzer (TGA) data were collected by Perkin-Elmer DSC-6 and TGA-6. Measurements of polymer molecular weights were done on a Viscotek GPC system with a UV−vis absorption detector at ambient temperature using tetrahydrafuran as the solvent. Polystyrene standards were used for conventional calibration.

Cyclovoltammetry. Electrochemical studies were performed on a Bioanalytical (BAS) Epsilon-100w trielectrode cell system. Three electrodes are a Pt working electrode, an ancillary Pt electrode, and a silver reference electrode (in a CH_3CN solution of 0.01 M $AgNO_3$ and 0.1 M tetrabutylammonium hexafluorophosphonate, TBA-HFP). The polymer samples were dissolved in hot solvents (such as *o*-dichlorobenzene) and then coated onto Pt working electrode. The measurements were performed in 0.1 M TBA-HFP/acetonitrile solution purged with nitrogen gas. Between the experiments, the surfaces of the electrodes were cleaned or polished. Scan rate was 100 mV/s. Ferrocene (2 mM in 0.10 M TBA-HFP/CH_3CN solution) was used as an internal reference standard, and its HOMO level of −4.8 eV was used in calculations.

2,5-Bisbromomethyl-3,4-dihexylthiophene (2). To a 125 mL round-bottom flask were added 2,5-dihexylthiophene (2.67 g, 10.6 mmol), paraformaldehyde (0.952 g, 31.7 mmol), acetic acid (25

* To whom correspondence should be addressed.
† Center for Material Research.
‡ Chemistry Department.

10.1021/ma802621b CCC: $40.75
Published on Web 01/13/2009

Scheme 1. Synthesis of PTV Derivatives with Sulfone Embedded in Polymer Conjugated Backbones

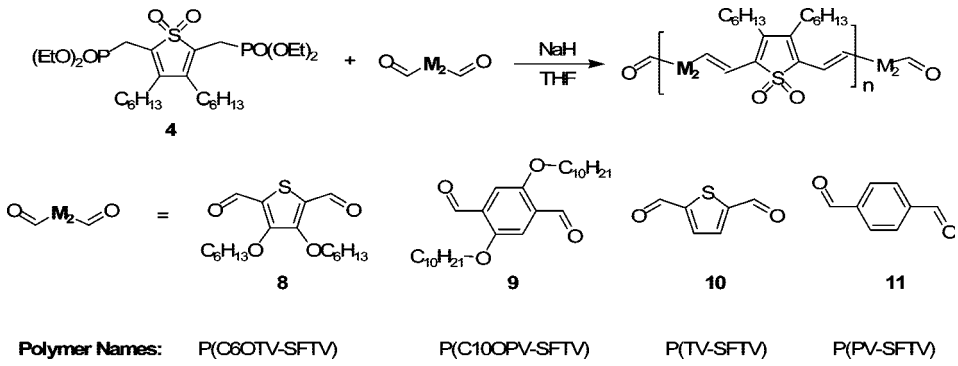

mL), 4.92 g of HBr in 30% acetic acid, and a stirring bar. The mixture was stirred at room temperature for 3 h. The mixture was poured into 30 mL of water and 30 mL of hexane in a separation funnel. Saturated aqueous $NaHCO_3$ was added to adjust the water phase to weakly basic. The top organic layer was collected, dried with $MgSO_4$, filtered, and condensed by vacuum rotary evaporation with water bath temperatures controlled near 40 °C. Heating was stopped immediately once the solvent was mostly removed to minimize decomposition of the product. The yield was 86% (4 g). The product could not be purified but was sufficiently pure for use in the next step. ^{1}H NMR ($CDCl_3$): δ (ppm) 0.90 (t, 6H, $-(CH_2)_4CH_3$), 1.33−1.52 (m, 16H), 2.51 (t, J = 7.7 Hz, 4H), 4.65 (s, 4H). (The spectrum is given in the Supporting Information.)

2,5-Di(bisethoxyphosphorylmethyl)-3,4-hexylthiophene (3). In a glovebox, a mixture of 2,5-dibromomethyl-3,4-dihexylthiophene (4 g, 9.1 mmol) and triethyl phosphite (6.05 g, 36.4 mmol) was stirred in a 125 mL round-bottom flask at 135 °C for 6 h. The remaining $P(OEt)_3$ was removed by vacuum distillation, and a light blue oil was obtained: 4.94 g, yield 98%. ^{1}H NMR ($CDCl_3$): δ (ppm) 0.90 (t, J = 6.6 Hz, 6H), 1.35−1.75 (m, 28H), 2.45 (t, J = 6.8 Hz, 4H), 3.28 (d, J = 19.2 Hz, 4H, $CH_2PO(EtO)_2$), 4.06 (quadruplet, J = 7.3 Hz, 8H). ^{13}C NMR ($CDCl_3$): δ (ppm) 14.10, 16.39, 22.64, 25.6, 27.27, 29.59, 30.65, 31.69, 62.29, 124.15, 139.61. (The spectra are given in the Supporting Information.)

2,5-Di(bisethoxyphosphorylmethyl)-1,1-dioxo-3,4-hexylthiophene (4). To a 100 mL round-bottom flask were added 2,5-di(bisethoxyphosphorylmethyl)-3,4-dihexylthiophene (2.48 g, 4.5 mmol) and *m*-chloroperoxybenzoic acid (3.165 g, 18 mmol), CH_2Cl_2 (20 mL), and a stirring bar. The mixture was stirred at room temperature for about 2 h. CH_2Cl_2 was removed by rotary evaporation at 40 °C under reduced pressure. The residue was diluted with 30 mL of hexanes and kept in a freezer for 2 days. The mixture was filtrated to collect the liquid part which was transferred into a separation funnel. An aqueous solution of Na_2CO_3 was added to make the water phase very basic. The hexane phase was collected, dried, and condensed. The crude product mixture was purified by column chromatography (125 mL silica gel, 1:2 ethyl acetate/hexanes) to give 1.3 g of product, 49.4% yield. ^{1}H NMR ($CDCl_3$): δ (ppm) 0.90 (t, J = 6.6 hz, 6H), 1.32−1.66 (m, 28H), 2.45 (t, J = 6.21 Hz, 4H), 3.00 (d, J = 20.91 Hz, 4H), 4.15 (quintet, J = 7.73 Hz, 8H). ^{13}C NMR ($CDCl_3$): δ (ppm) 14.01, 16.31, 20.60, 22.49, 26.11, 28.28, 29.53, 31.44, 62.82, 127.55, 142.64. (The spectra are given in the Supporting Information.) Anal. Calcd: C, 53.41; H 8.62; S, 5.48; Found: C, 53.29; H, 8.69; S, 5.62.

3,4-Bishexyloxythiophene (6). To a two-neck round-bottom flask equipped with a thermometer were added 3,4-dimethoxythiophene (12.49 g, 86.7 mmol), anhydrous hexanol (35.56 g, 0.384 mol), and *p*-toluenesulfonic acid monohydrate (0.5 g, 2.61 mmol). The mixture was stirred at 90−95 °C for 25 h with vacuum applied occasionally to remove side product methanol to drive the reaction to completion. The mixture was poured into a 1 L separation funnel. Dilute HCl was added to neutralize the mixture, which was then extracted with 100 mL of hexanes. The extract was dried with magnesium sulfate, filtered, condensed by rotary evaporation, and vacuum-distilled to 21.08 g of product with a 95% yield. ^{1}H NMR ($CDCl_3$): same as in ref 18.

2,5-Dibromo-3,4-bishexyloxythiophene (7). To a stirred mixture of 3,4-bishexyloxythiophene (7.0 g, 24.6 mmol) and *N*,*N*-dimethylformamide (anhydrous, 38 mL) in the dark, *N*-bromosuccinimide (9.63 g, 54.1 mmol) in 100 mL of DMF was added over 2 h from an addition funnel. One hour after the addition, the mixture was transferred into a 500 mL separation funnel and diluted with 30 mL of water. The mixture was extracted with 100 mL of hexanes. The extract was collected, dried with magnesium sulfate, filtered, and condensed. The residue was purified by a silica gel column using hexanes as the eluent to afford 6.64 g of oil with a yield of 61%. ^{1}H NMR ($CDCl_3$): δ (ppm) 0.90 (t, 6H), 1.32 and 1.45 (m, 16H), 1.72 (quintet, J = 6.6 Hz, 4H), 4.05 (t, J = 6.8 Hz, 4H). ^{13}C NMR ($CDCl_3$): δ (ppm) 14.05, 22.62, 25.53, 29.90, 31.57, 73.94, 95.25, 147.59. The spectra are given in the Supporting Information.

2,5-Dialdehyde-3,4-bishexyloxythiophne (8). To a mixture of *n*-BuLi (1.6 M in hexane, 26.7 mL, 42.8 mmol) and THF (67 mL) cooled in dry ice/hexane bath, a solution of 2,5-dibromo-3,4-bishexyloxythiophene (6.30 g, 14.3 mmol) in 10.0 mL of THF was added slowly through a syringe. Two minutes later, DMF (anhydrous, 3.33 g, 45.6 mmol) was added, and the mixture was warmed to room temperature and poured into a separation funnel that contained 67 mL of water and 67 mL of hexanes. After usual work-up, the crude product was purified by silica gel column chromatography using 1:17 ethyl acetate:hexanes mixture as the eluent to afford 3.90 g of pure product with a yield of 80%. ^{1}H NMR ($CDCl_3$): δ (ppm) 0.91 (t, 6H), 1.33&1.46 (m, 16H), 1.80 (quintet, J = 6.8 Hz, 4H), 4.27 (t, J = 6.6 Hz, 4H), 10.10 (s, 2H). ^{13}C NMR ($CDCl_3$): δ (ppm) 182.19, 154.98, 131.17, 75.67, 31.46, 29.83, 25.44, 22.55, 13.99. The spectra are given in the Supporting Information. ^{1}H NMR peaks are same as reported (though the literature data[18] were not as detailed as presented here).

Poly(3,4-bishexyloxythienylenevinylene-*S*,*S*-dioxide-3′,4′-dihexylthienylenevinylene), P(C6OTV-SFTV). In a glovebox, NaH (20.1 mg, 0.837 mmol) in 10 mL vial with 4 mL of THF was added dropwise to a stirred solution of **4** (213.5 mg, 0.365 mmol) and comonomer **8** (116.4 mg, 0.342 mmol) in 2 mL of THF in a 20 mL flask at room temperature. Twenty-one hours later, a few drops of acetic acid were added to neutralize the solution. The solution was dropped into stirred methanol. The resulting dark blue polymer solid was collected by filtration, washed with methanol many times, and dried in air a day and in vacuum at 65 °C for 24 h. Yield: 0.135 g, 58%. ^{1}H NMR ($CDCl_3$): δ (ppm) 0.93 (m. 12H), 1.36 (m, 28H), 1.79 (m, 4H), 2.45 (t, 4H), 4.12 (s, 4H), 6.69 (d, J = 16 Hz, 2H), 7.45 (d, J = 16 Hz, 2H). ^{13}C NMR ($CDCl_3$): δ (ppm) 14.1, 22.63, 25.62, 29.4, 30.07, 31.56, 74.37, 112.29, 123.40, 125.88, 135.50, 138.39, 149.86. (Some aliphatic carbon peaks are overlapped.)

Poly(thienylenevinylene-*S*,*S*-dioxo-3′,4′-dihexylthienylenevinylene), P(TV-SFTV). To a solution of 2,5-thiophenedicarboxaldehyde (50.3 mg, 0.359 mmol) and **4** (200.0 mg, 0.342 mmol) in THF (2 mL), NaH (18.9 mg, 0.788 mmol) in 3 mL of THF was

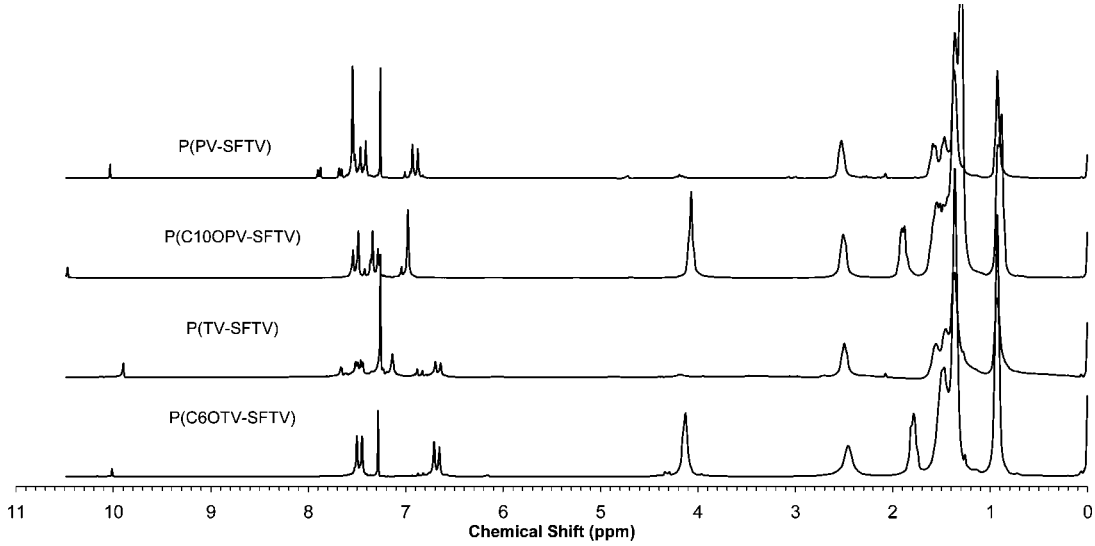

Figure 1. ^{1}H NMR of P(C10OPV-SFTV), SF-PTV, P(TV-SFTV), and P(PV-SFTV) in $CDCl_3$ at 65 °C. The last two polymers are not fully dissolved; thus, the solutions have higher content of low-MW polymers and higher content of end groups (−CHO).

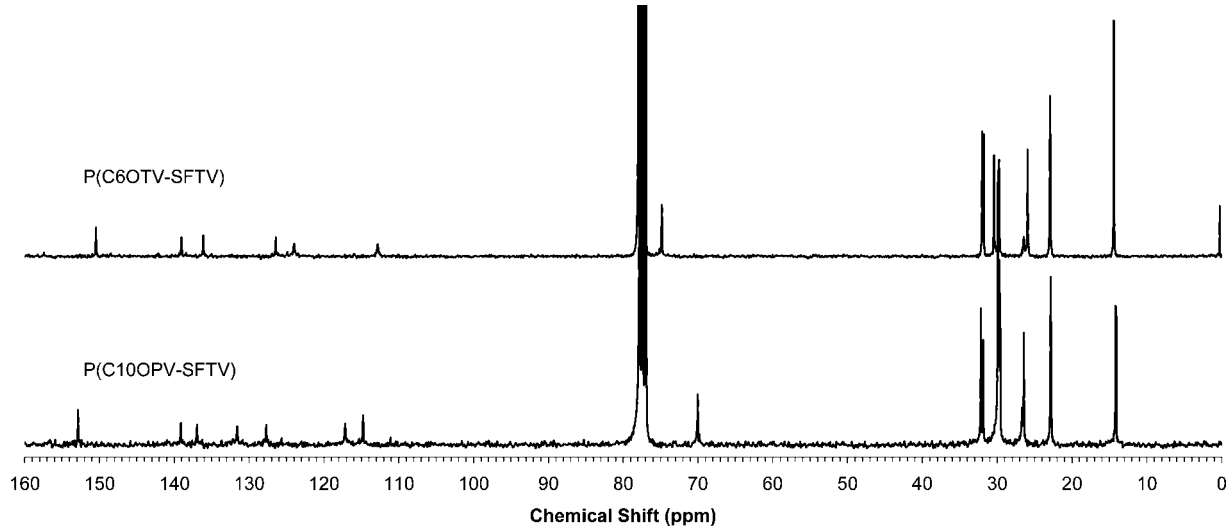

Figure 2. ^{13}C NMR spectra of P(C10OPV-SFTV) and P(C6OTV-SFTV) in $CDCl_3$ at 65 °C. The solubilities of the other two polymers are not high enough to obtain good ^{13}C NMR spectra.

added dropwise. No immediate color change upon NaH addition was observed. Twenty-two hours after addition, the blue reaction solution was dropped into MeOH (30 mL, acidified with 60 mg of HOAc). The polymer product was collected by filtration and was dried in vacuo at 50 °C for 10 h to afford 127 mg of black powder. Yield: 81.5%. The ^{1}H NMR spectrum is shown in Figure 1.

Poly(1,4-phenylenylenevinylene-*S,S*-dioxo-3′,4′-dihexylthienylenevinylene), P(PV-SFTV). The same procedure as used for P(TV-SFTV) and the same amount (in mmol) of monomers were used. Yield: 133 mg, 93.3%. The ^{1}H NMR spectrum is shown in Figure 1.

Poly(2,5-bisdodecyloxy-1,4-phenylenylenevinylene-*S,S*-dioxo-3′,4′-dihexylthienylenevinylene), P(C10OPV-SFTV). The same procedure as used for P(TV-SFTV) and same amounts (no. of mmol) of monomers were used. Yield: 205 mg, 80%. ^{1}H and ^{13}C NMR spectra are in Figures 1 and 2. ^{1}H NMR ($CDCl_3$): δ (ppm) 0.92 and 0.88 (terminal CH_3 of hexyl and dodecyl respectively, m, 12H), 1.1−1.7 (m, 44H), 1.90 (m, 4H), 2.50 (t, 4H), 4.06 (t, J = 6.6 Hz, 4H), 7.03 (s, 2H), 7.30 (d, J = 16.5 Hz, 2H), 7.50 (d, J = 16.2 Hz, 2H), 10.44 (terminal CHO). ^{13}C NMR ($CDCl_3$): δ (ppm) 14.15, 22.91, 26.46, 26.72, 29.60, 29.76, 29.89, 29.93, 31.90, 32.20, 69.94, 114.58, 116.97, 127.51, 131.39, 136.73, 138.88, 152.59. (Several aliphatic carbon peaks overlapped.)

3. Results and Discussion

3.1. Synthesis of Monomers and Polymers. The structures of the series of *S,S*-dioxide-thienylenevinylene-based polymers [P(C6OTV-SFTV), P(C10OPV-SFTV), P(TV-SFTV), and P(PV-SFTV)] and their generic synthetic scheme are shown in Scheme 1. The polymers were prepared from two types of comonomers: the diphosphonate **4** and aromatic dialdehydes (**8**, **9**, **10**, and **11**) via the Horner−Emmons reaction. The diphosphonate monomer (**4**) was synthesized in four steps from 3,4-dibromothiophene (Scheme 2). Compound **1** was synthesized according to the literature procedure.[13] Compound **2** was obtained from bromomethylation of **1** under reaction condition similar to what was recently reported.[14] Better yield (86% vs 75%) was obtained as a result of more detailed study of the reaction. We found that the reaction was very fast and was completed in less than 3 h. However, care must be taken during work-up because the product **2** is highly unstable and can decompose during solvent rotary evaporation when the temperature was above 50 °C. The crude product was pure enough to give a neat ^{1}H NMR spectrum (Figure 1 in the Supporting Information (SI)) showing a characteristic singlet peak at 4.65 ppm for two $-CH_2Br$

Scheme 2. Synthesis of the Diphosphonate Comonomer 4

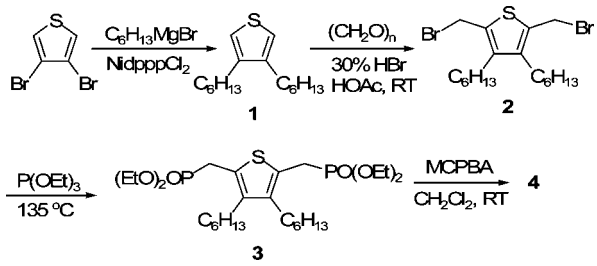

Scheme 3. Synthesis of the Dialdehyde Comonomer 8

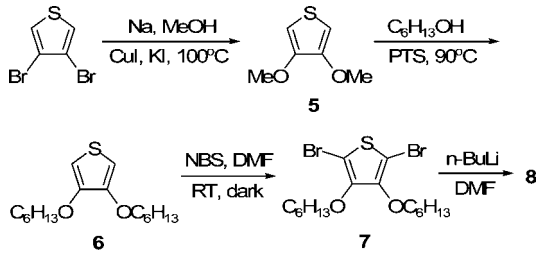

groups. **2** is not stable in silica gel column, so the crude product was used in the next step. Instability of **2** at elevated temperatures did not cause any problems in the next step in the Michaelis−Arbuzov reaction[15] run at 135 °C. Product **3** has a characteristic doublet at 3.20 ppm in the ^{1}H NMR spectrum. Purification of **3** by silica gel column chromatography was attempted, but decomposition happened in the column, as a substantial amount of new substance (not present in crude product) was found in collected fractions.[16] The crude product (95% pure, see ^{1}H NMR in Figure 1 in SI) was oxidized at the sulfur atom using a literature procedure[12] to give product **4**, which was stable and was purified by column chromatography to give pure product at 49% overall yield for three steps. The ^{1}H NMR spectrum of **4**, also shown in Figure 1 in the Supporting Information, is characterized by a doublet peak at 2.97 ppm for $CH_2PO(OCH_2CH_3)_2$ which was shifted from 3.20 ppm in **3** due to vanishing of the deshielding effect of the thiophene ring as a result of loss of aromaticity of the thiophene ring.[17]

Synthesis of dialdehyde monomer (**8**) took four steps using a scheme (Scheme 3) different from the one reported in 1999.[18] Compound **5** was synthesized according to a literature procedure.[19] Compound **6** was synthesized from **5** by PTS-catalyzed substitution of methoxy by a hexyloxy group at 90 °C. The literature procedure[20] was followed, except that the reaction was conducted under a reduced pressure (400−500 mbar) instead of 1 atm to constantly remove the side product methanol from the reaction system. With this modification we were able to improve the yield from 54% to 95%. Compound **7** was synthesized from **6** by dibromination and was characterized by the disappearance of the peak at 6.15 ppm in the ^{1}H NMR spectrum (Figure 3 in Supporting Information). Finally, the comonomer **8** was obtained from **7** by diformylation in 80% yield (^{1}H and ^{13}C NMR spectra in Figures 3 and 4 in Supporting Information). It is noted that errors are found in the literature NMR data.[21]

The polymerization reaction for P(C6OTV-SFTV) was performed inside a glovebox. Initially, 1 equiv of potassium *tert*-butoxide base was used, the blue color appeared within 1 h, the reaction progress was followed by ^{1}H NMR analysis, and >30% of both monomers remained no matter how long the reaction was allowed to run. Clearly, the base was partially consumed by side reactions. When more and more *t*-BuOK was added, the characteristic blue-green color of formed oligomers/polymer started to fade even before aldehyde and phosphonate were completely consumed. The color change and NMR data suggested that the double bonds formed in the earlier stage of the reaction were destroyed extensively by the base (now acting as a neucleophile) through the Michael addition reaction (a nucleophilic conjugate addition). The similar side reaction was reported in the synthesis of CN-PPV.[22] We found that the decomposition could be avoided by using sodium hydride of strictly controlled amount. The deep green polymer products could be obtained routinely. For the ^{1}H NMR in Figure 1 (bottom), 5% excess of aldehyde monomer was used to control the molecular weight. The phosphonate monomer is fully consumed as indicated by the disappearance of the doublet at 2.97 ppm. The residue aldehyde peak is seen in the spectrum as expected. Two clean doublets at 6.69 and 7.45 ppm, due to the two nonidentical protons in the newly formed C═C bond, indicate low content of structural defects.

The other three polymers were synthesized from monomer **4** and dialdehydes **9**,[5] **10**, and **11**, respectively, using similar condition as used for the synthesis of P(C6OTV-SFTV). The ^{1}H NMR spectra of these polymers are shown in Figure 1. In the spectrum of P(C10OPV-SFTV), a singlet at 6.98 ppm (due to two identical phenyl protons) and two doublets at 7.30 and 7.50 ppm (due to the newly formed C═C bond) are as clean as the aromatic peaks in the P(C6OTV-SFTV) spectrum. The same combination of aromatic peaks (one single and two doublets) is seen for the other two polymers, P(TV-SFTV) and P(PV-SFTV), with different chemical shifts. However, the peaks due to the terminal aromatic units and aldehyde groups in the spectra of P(TV-SFTV) and P(PV-SFTV) are stronger than the corresponding peaks in the spectra of the other two polymers. This difference is simply due to the fact that P(TV-SFTV) and P(PV-SFTV) have much lower solubility due to fewer side chains, and the dissolved portions in the NMR sample tubes are mostly of low MW and had higher content of terminal units. The solubility of P(C6OTV-SFTV) is good in common organic solvents such as THF (1 mg/1 mL) and chloroform (2 mg/1 mL) at room temperature. P(C10OPV-SFTV) is about half as soluble as P(C6OTV-SFTV). Decent ^{13}C NMR spectra were obtained for these two polymers (Figure 2), and correct counts of aromatic carbon peaks are obtained. The peaks due to terminal units are not observed due to their relatively weak intensities.

Molecular weights of SF-PTVs were measured by GPC. It was found that the refractive index detector signal was severely distorted by the strong absorption of SF-PPVs. An absorption detector was then used in place of the original RI detector. The results are listed in Table 1. Because of the nonstoichiometric use of the two comonomers and small scale of the reactions, the MWs are not high. In the case of P(PV-SFTV) and P(TV-SFTV), measured MWs were particularly low because only the low-MW fractions were dissolved and tested. The reaction scale also affects molecular weight of synthesized polymers, as the amount of NaH is very small for small scale reactions. In a larger scale synthesis of P(C6OTV-SFTV), in which the amount of diphosphonate **4** was increased from 231 mg to 1.62 g, the number-average MW (M_n) increased to 16 800 (calculated from the proton integration ratio of CHO and OCH_2 peaks), which is very close to the value (13 590) calculated from the feed ratio of the two monomers (1.05:1 was used) since some of the low-MW fraction was lost during the precipitation/filtration process. GPC measurement gave a M_w of 47.7K, a M_n of 21.7K, and a PDI of 2.20. The M_n is higher than the result calculated from ^{1}H NMR integrations, as expected.

3.2. Thermal Properties Analyzed by DSC, TGA, and NMR. In sulfone-containing polymers, due to the relatively weak C−S bonds, thermally induced chemical decomposition

Table 1. Molecular Weight and Thermal Properties of the Sulfone Polymers

	M_w/M_n/PDI	onset T (K) of endothermic decomposition (DSC)	onset T (K) of exothermic peaks (DSC)	onset T (K) for loss of SO_2 (TGA)
P(PV-SFTV)	5350/2880/1.84	280−295	298	292
P(TV-SFTV)	3570/1700/2.10	290	258	258
P(C10OPV-SFTV)	13.6K/5.44K/2.50	290	260	264
P(C6OTV-SFTV)	11.5K/4.34K/2.66	264		266

usually begins with the loss of SO_2.[23] DSC, TGA, and ^{1}H NMR were used to study the decomposition behaviors of the SF-PTVs. DSC scans of the polymers are shown in Figure 3. In the low temperature range (RT−250 °C), P(C10PV-SFTV) and P(TV-SFTV) undergo a weak exothermic transition at 115 and 117 °C, respectively. They are most likely due to reorganization of side chains. All polymers except P(C6OTV-SFTV) show an endothermic peak above 250 °C with onset temperatures listed in Table 1. To determine whether the endothermic process is due to melting or decomposition (loss of SO_2), we selected P(C10OPV-SFTV) for detailed study because its good solubility allows for easy NMR analysis. First, a sample of this polymer was heated quickly in DSC under a N_2 atmosphere to 250 °C (at a rate of 30 °C/min) and was held at this temperature for 1 min. After cooling to RT, the sample was still in the powder form. ^{1}H NMR of the sample showed no decomposition. Another sample of P(C10OPV-SFTV) was heated to 290 °C (the completion temperature of the endothermic peak) and was let cool immediately. The sample was found still in powder form but was only partially soluble in boiling $CDCl_3$. ^{1}H NMR of the soluble part (Figure 4) revealed that the polymer was completely changed (no original aromatic peak seen); however, C10OPV unit and two C_6H_{13} side chains (attached to C═C bond) remained. These observations suggest that the endothermic peak (with an onset at 264 °C) is not due to melting but due to disintegration (most likely loss of SO_2).

The TGA experiment of P(C10OPV-SFTV) (Figure 5) shows a weight loss onset temperature of 264 °C, matching well with the endothermic onset temperature. In the DSC curve of P(C10OPV-SFTV) as well as that of P(TV-SFTV), the endothermic process was overpowered by an exothermic transition (due to reactions involving unsaturated bonds). In the case of P(PV-SFTV) and P(C6OTV-SFTV), the exothermic decomposition processes (by DSC) are coincident with disintegration

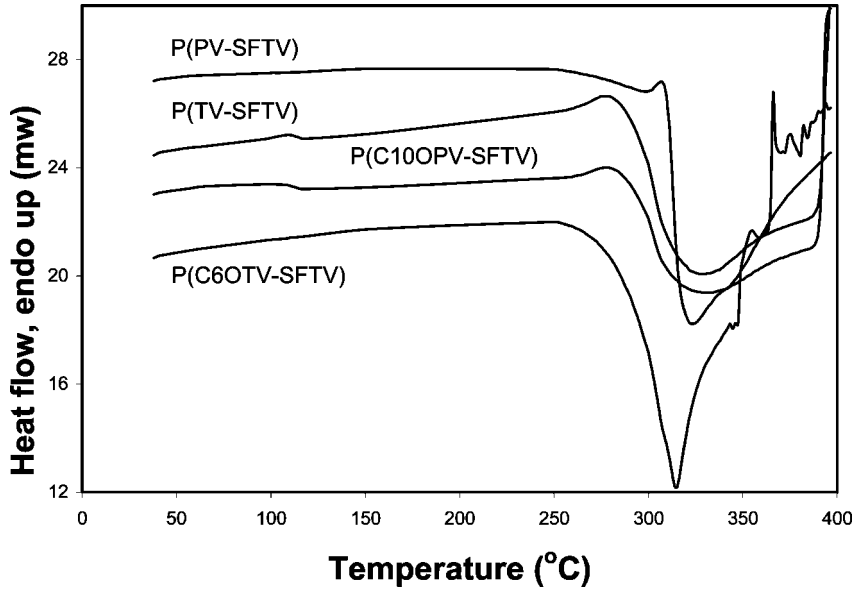

Figure 3. DSC curves of four sulfone-PTVs.

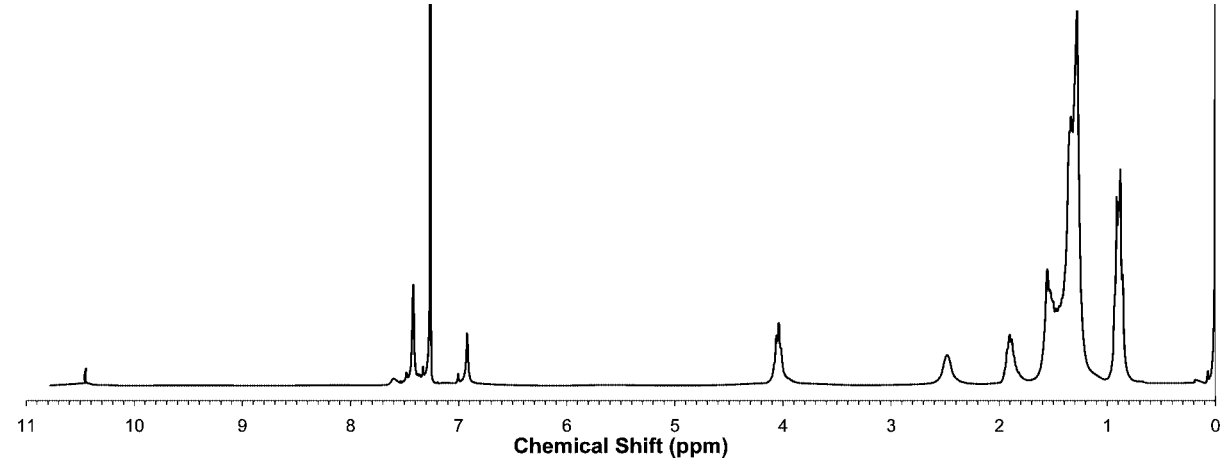

Figure 4. ^{1}H NMR ($CDCl_3$) spectrum of a P(C10OPV-SFTV) sample heated to 290 °C (DSC, N_2, heating rate 10 °C/min, no stay at 290 °C).

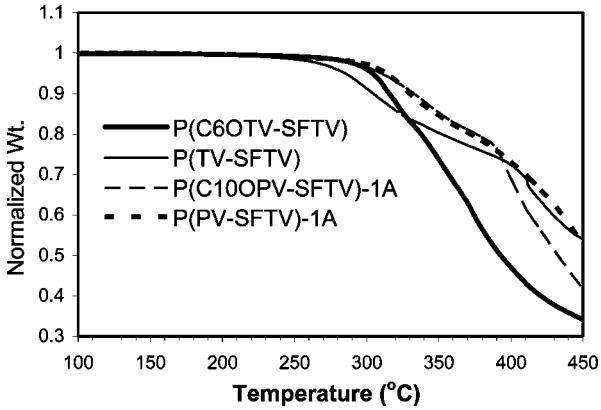

Figure 5. Thermal gravity analysis (TGA) for SF-PTVs.

(weight loss) processes (by TGA), indicating that the heat released from cross-linking reactions of C═C bonds can fully compensate for the heat needed for disintegration reactions (e.g., loss of SO_2) (except for a short temperature range of 300−310 °C in the case of P(PV-SFTV)).

No melting behaviors of these polymers were observed before their decomposition temperatures. The electron-withdrawing sulfone group should impart good oxidation stability to these polymers. P(C6OTV-SFTV), the most electron-rich among the four, was selected for a static heating test at 160 °C in air for 30 min. The heated sample did not decompose at all as indicated by its ^{1}H NMR spectrum. From the DSC and TGA data presented in Table 1, we conclude that the sulfone-based polymers are dynamically stable to temperatures as high as 258 °C.

3.3. Optical and Electrochemical Properties. Figure 6 (top) shows the absorption spectra of the SF-PTV solutions of the same nominal concentration (0.1 mM in chloroform, boiled, then cooled to RT). The absorption tails of P(C10OPV-SFTV) and P(C6OTV-SFTV) vanishes quickly at the long wavelength side, indicating that the two polymers were fully dissolved. The peak absorbance of the two polymer solutions are 3.11 and 3.27, very close to each other with a difference of ±2.5% from the average value. In the spectra of the other two polymers, the absorption peaks sit on a slope. The slope, higher at the short wavelength side, is due to light scattering by insoluble polymer particles or precipitate. The two solutions were then filtered with 0.2 μm filters, and absorption spectra of the resulting solutions were obtained. By comparing the peak absorbance (1.10 and 0.753) of the filtered solutions with the average peak absorbance (3.19) of the two fully dissolved polymers, we get estimated solubility of 0.034 mM (15 mg/L) and 0.024 mM (9.7 mg/L) for P(TV-SFTV) and P(PV-SFTV), respectively. Normalized absorption spectra of four polymers solutions (fully dissolved or filtered) are shown in Figure 6 (bottom). The absorption ranges of four polymers span over the full visible range. The absorption λ_{max} and optical energy gaps (E_g^{opt}s, calculated from absorption cutoff wavelengths) are listed in Table 2. The energy gap decreases as the donor unit changes from simple phenylene all the way to 3,4-bishexyloxythienylene, with a good correlation with aromatic resonance energy and electronic richness of the aromatic unit.

Photoluminescent measurements were performed for both solutions and films of the polymers; no PL signal was detected for any of the samples. This result is consistent with the nonfluorescent nature of various PTV-based polymers.[9,11,24]

Electrochemical measurements were performed for SF-PPVs in thin films coated on Pt working electrode (Figure 7). LUMO/HOMO levels are estimated from the redox potentials (Table 2) and corresponding electrochemical energy gaps (E_g^{EC}s) are

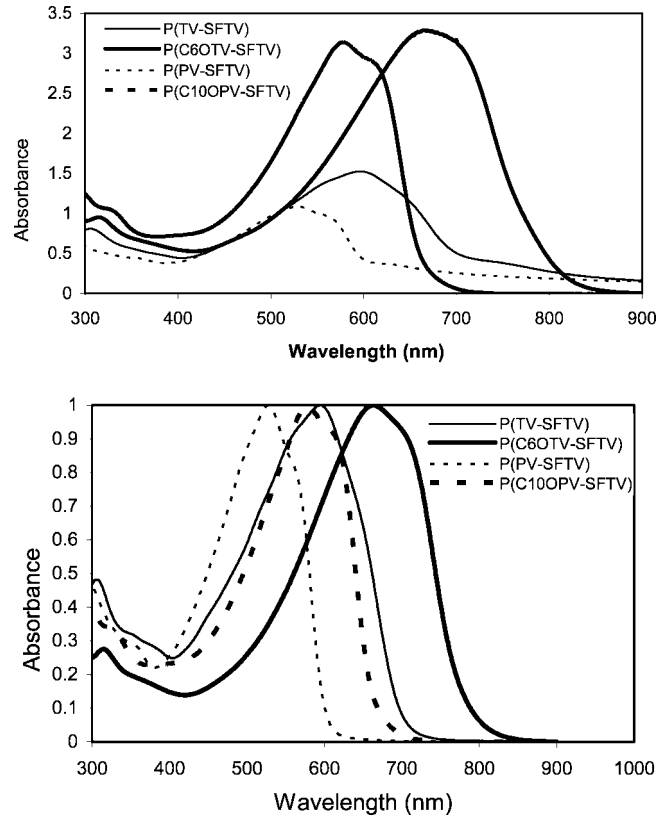

Figure 6. Top: UV−vis absorpton spectra of SF-PTV chloroform solutions with nominal concentration of 0.1 mM without filtration. The latter two polymers are not fully dissolved. Scattering of light by the polymer particles is evident in the spectra of these two polymers. Bottom: normalized UV−vis absorption spectra of above solutions. P(TV-SFTV) and P(PV-SFTV) solutions were filtered with 0.1 μm filter.

also listed in Table 2. The LUMO levels of all SF-PTVs are very close (with differences <0.1 eV). This is consistent with the fact that the acceptor unit is the same for all SF-PTVs and that the LUMO level is mostly affected by electron-withdrawing group(s) of the π-conjugated systems.[7,25] The SF-PTVs are similar to the well-known acceptor polymer CN-PPV[26] in terms of the LUMO level and are likely to function as acceptors when paired with electron-rich π-conjugated polymers. Because of the fact that SF-PTVs have lower E_gs and are not luminescent, photoluminescence quenching may not be soly used to confirm the photoinduced charge transfer in the blend of SF-PTV with commonly used donor polymers. Other types of experiments (such as ESR, PIA, and photoconductivity) should be conducted to confirm the acceptor nature and photovoltaic potentials of these polymers (especially the two soluble polymers).

3.4. Computational Study of HOMO/LUMO Levels and Energy Gaps. *3.4.1. Design of Model Structures.* The optical energy gap of P(C6OTV)-SFTV) is 1.54 eV (in chloroform), which is ∼0.3 eV lower than the regular monoalkyl-substituted PTV.[10] The reduction in E_g could be attributed to two factors: (1) the loss of aromaticity of the second thiophene unit and (2) the donor−acceptor interaction between the sulfone acceptor and alkoxy-substituted thiophene donor in the π-conjugated system.[7] To determine which factor is dominant, we conducted computational study on three series of model oligomers (Figure 8): $(MeOT\text{-}TV)_n$, $(MeOT\text{-}4V)_{n=1-4}$, and $(MeOTV\text{-}SFTV)_{n=1-4}$. The latter two can be considered as the derivatives of the first structure. $(MeOT\text{-}4V)_n$ will allow us to see how much reduction in E_g could be produced by removing aromaticity of the second thiophene ring. $(MeOTV\text{-}SFTV)_n$ has the same backbone as

Table 2. Electronic Properties of SF-PTVs

	λ_{max} (nm) ($CHCl_3$/film)	λ_{max} (nm) of PL in $CHCl_3$	$\lambda_{cutoff}/E_g^{opt}$ (nm/eV)	onset redox potentials (V vs Ag/Ag^+)	LUMO/HOMO/ E_g^{EC} (eV)
P(PV-SFTV)	528/495	550	608/2.04	−1.26/0.80	−3.48/−5.54/2.06
P(C10OPV-SFTV)	578/595		684/1.82	−/0.49	−/−5.23/−
P(TV-SFTV)	594/635		708/1.75	−1.18/0.62	−3.56/−5.36/1.80
P(C6OTV-SFTV)	663/616		806/1.54	−1.20/0.42	−3.54/−5.16/1.62

P(C6OTV-SFTV). Computation of energy gaps of this series of model oligomers will allow us to find how much additional reduction in energy gap can be obtained by replacing the CH_2 unit with a SO_2 unit.

3.4.2. Computational Method. HOMO/LUMO energy levels and E_gs were obtained by quantum mechanical calculation of oligomers with increasing length and followed by extrapolation of calculated values to infinite chain length.[27] Hybrid exchange-correlation functional B3LYP in the density functional theory (DFT) formalism was used for both geometry optimization and energy calculation, where B3LYP stands for Becke's three-parameter hybrid functional using the Lee−Yang−Parr (LYP) correlation functional.[28] As shown by Yang et al.,[27] B3LYP (for both geometry optimization and energy level calculation) is one of the best methods for estimating E_gs for PTV polymers under an appropriate computational cost. Considering the computational power available, small basis set 3-21G* was used and implemented in Gaussian 03.[29] The E_gs of polymers were obtained by plotting the E_gs of monomers through tetramers against reciprocal of the number of double bonds on the main chain and extrapolating the fitting line to the infinite number of double bonds, according to the free-electron molecular orbital model (FEMO).[30]

3.4.3. Computational Results and Discussion. The results of HOMO/LUMO and E_gs for the three series of oligomers are listed in Table 3. The E_g values are plotted in Figure 9 as functions of $1/m$, where m is the number of C=C double bonds in the oligomers. Extrapolation of the linear fitting lines results

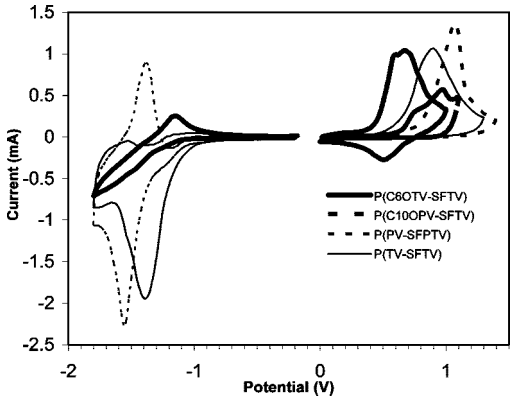

Figure 7. Cyclic voltamograms of SF-PTV films coated on Pt wire. Reference electrode: Ag in 0.1 M $AgNO_3$/MeCN.

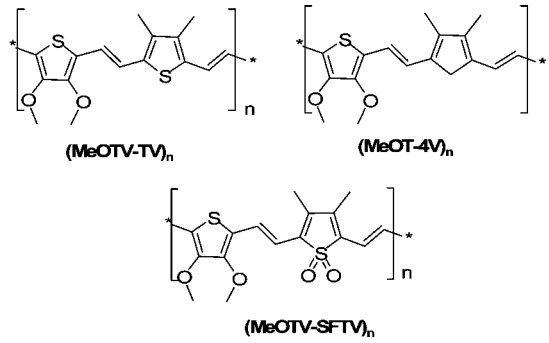

Figure 8. Model structures for DFT computational study.

Table 3. Results of DFT Calculations

		LUMO (eV)	HOMO (eV)	E_g (eV)
$(MeOT\text{-}TV)_n$	$n = 1$	−1.496	−4.76	3.264
	$n = 2$	−1.9856	−4.3792	2.3936
	$n = 3$	−2.176	−4.2432	2.0672
	$n = 4$	−2.2576	−4.1888	1.9312
	$n = \infty$			1.4855
$(MeOT\text{-}4V)_n$	$n = 1$	−1.4416	−4.5152	3.0736
	$n = 2$	−1.9312	−4.1072	2.176
	$n = 3$	−2.0944	−3.9712	1.8768
	$n = 4$	−2.176	−3.9168	1.7408
	$n = \infty$			1.2784
$(MeOTV\text{-}SFTV)_n$	$n = 1$	−2.2848	−5.2496	2.9648
	$n = 2$	−2.8288	−4.9504	2.1216
	$n = 3$	−2.992	−4.7872	1.7952
	$n = 4$	−2.992	−4.5968	1.6048
	$n = \infty$			1.2313

in E_gs of polymers ($n = \infty$) which are also listed in Table 3. The obtained E_g for $(MeOTV\text{-}SFTV)_{n=\infty}$ is 1.19 eV, smaller than the experimental value of 1.54 eV obtained for P(C6OTV-SFTV) in chloroform solution. The underestimation is consistent with the literature report[27] that the combination of B3LYP/B3LYP at DFT level usually produces E_g lower than experimental results for PTV and other conjugated systems. The E_g of $(MeOTV\text{-}4V)_n$ is smaller than that of $(MeOT\text{-}TV)_n$ by 0.2 eV, suggesting that the removal of aromaticity is effective in reducing E_g. But from $(MeOTV\text{-}4V)_n$ to $(MeOTV\text{-}SFTV)_n$, E_g only decreases by 0.097 eV. The results suggest that the low E_g of P(C6OTV-SFTV) is mainly due to the loss of the aromaticity of the thiophene. Since the donor units in other three synthesized polymers are less electron rich, the contributions from D−A interactions should be even less. Although the sulfone group in $(MeOTV\text{-}SFTV)_n$ is not very effective in reducing E_g, it does bring LUMO down significantly by ~0.7 eV with respect to those of $(MeOTV\text{-}4V)_n$, making SF-PTVs potentially useful as electron acceptors in variety of polymer electronic and optoelectronic applications.

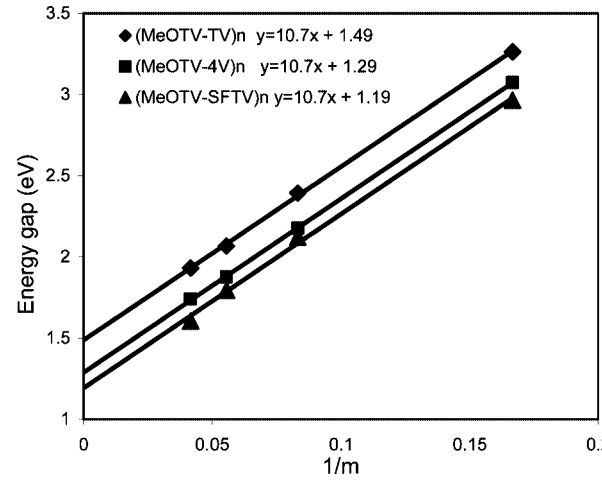

Figure 9. Plots of calculated energy gaps versus $1/m$ where m is the total number of C=C bonds in each oligomer. Linear fitting of the data points of each series and extrapolation of the fitting lines are also shown.

4. Conclusions

A series of conjugated main-chain terminal functionalized and evolving energy gap sulfone-containing thienylenevinylene-based copolymers have been developed and studied. The HOMO/LUMO energy gaps of these polymers were in the range 1.5−2.0 eV. Oxidation of one of every two thiophene units brings about 0.3 eV in reduction in energy gap. Two-thirds or more of the energy gap reduction can be attributed to the removal of aromaticity of the thiophene ring, and the rest is due to the donor−acceptor interaction between the sulfone and RO-substituted thiophene ring. The sulfone group greatly lowers both HOMO/LUMO levels, making these polymers potential electron acceptors (n-type) for polymeric electronic/optoelectronic applications. Lowering HOMO/LUMO levels also improve the air stability of the materials. The sulfone polymers have dynamic stability at 258 °C or higher, and the decomposition starts with loss of polymer components in contrast to regular PTVs which decompose initially by cross-linking. The well-defined terminal functional groups (aldehyde or phosphonate) make these polymers potentially ideal acceptor polymer blocks for the development of D−A block copolymer supramolecular nanostructures.[5]

Acknowledgment. This material is based upon work supported, in part, by the Department of Defense under Awards HQ0006-07-C-0017, W911NF-06-1-0488, and FA8650-07-C-5058 and by NASA under Award NAG3-1035. We thank Alexander Gavrilenko for help on the Gaussian program.

Supporting Information Available: ^{1}H and ^{13}C NMR spectra of all the precursors to the two monomers. This material is available free of charge via the Internet at http://pubs.acs.org.

References and Notes

(1) Sun, S., Sariciftci, S., Eds.; *Organic Photovoltaics: Mechanisms, Materials and Devices*; CRC Press: Boca Raton, FL, 2005 (ISBN: 978-0824759636).
(2) (a) Zhang, C.; Sun, S. Organic and Polymeric Photovoltaic Materials and Devices. In *Introduction to Organic Electronic and Optoelectronic Materials and Devices*; Sun, S., Dalton, L., Eds.; CRC Press/Taylor & Francis: Boca Raton, FL, 2008; Chapter 14, pp 401−420. (b) Sun, S. Organic and Polymeric Solar Cells. In *Handbook of Organic Electronics and Photonics*; Nalwa, S. H., Ed.; American Scientific Publishers: Los Angeles, CA, 2008; Vol. *3*, Chapter 7, pp 313−350.
(3) (a) Zhan, X.; Tan, Z.; Domercq, B.; An, Z.; Zhang, X.; Barlow, S.; Li, Y.; Zhu, D.; Kippelen, B.; Marder, S. R. *J. Am. Chem. Soc.* **2007**, *129*, 7246–7247. (b) Tan, Z.; Zhou, E.; Zhan, X.; Wang, X.; Li, Y.; Barlow, S.; Marder, S. R. *Appl. Phys. Lett.* **2008**, *93*, 073309.
(4) Scherf, U.; Gutacker, A.; Koenen, N. *Acc. Chem. Res.* **2008**, ASAP.
(5) Zhang, C.; Choi, S.; Haliburton, J.; Cleveland, T.; Li, R.; Sun, S.; Ledbetter, A.; Bonner, C. *Macromolecules* **2006**, *39*, 4317–4326.
(6) Sun, S.-S.; Zhang, C.; Ledbetter, A.; Choi, S.; Seo, K.; Bonner, C. E., Jr.; Drees, M.; Sariciftci, N. S. *Appl. Phys. Lett.* **2007**, *90*, 043117.
(7) Roncali, J. *Chem. Rev.* **1997**, *97*, 173–205.
(8) Loewe, R. S.; McCullough, R. D. *Chem. Mater.* **2000**, *12*, 3214, and references therein.
(9) Hou, J.; Tan, Z.; He, Y.; Yang, C.; Li, Y. *Macromolecules* **2006**, *39*, 4657–4662.
(10) Gavrilenko, A. V.; Matos, T. D.; Bonner, C. E.; Sun, S.-S.; Zhang, C.; Gavrilenko, V. I. *J. Phys. Chem. C* **2008**, *112*, 7908–7912.
(11) Synthesis and Characterization of Fully Regioregular Head-to-Tail Poly(3-Dodecyl-2,5-Thienylenevinylene) for Opto-Electronic Applications. Zhang, C.; Matos, T.; Li, R.; Maaref, S.; Annih, E.; Sun, S.-S.; Zhang, J.; Jiang, X. Submitted to *Chem. Mater.*
(12) Barbarella, G.; Favaretto, L.; Sotgiu, G.; Zambianchi, M.; Arbizzani, C.; Bongini, A.; Mastragostino, M. *Chem. Mater.* **1999**, *11*, 2533–41.
(13) Diaz-Quijada, G. A.; Weinberg, N.; Holdcroft, S.; Pinto, B. M. *J. Phys. Chem. A* **2002**, *106*, 1266–1276.
(14) Shahid, M.; Ashraf, R. A.; Klemm, E.; Sensfuss, S. *Macromolecules* **2006**, *39*, 7844–7853.
(15) Bhattacharya, A. K.; Thyagarajan, G. *Chem. Rev.* **1981**, *81*, 415–430.
(16) The decomposition of **3** was not mentioned in ref 14 but is likely the reason for unavailability of elemental analysis data.
(17) Günther, H. *NMR Spectroscopy: Basic Principles, Concepts, and Applications in Chemistry*, 2nd ed.; John Wiley & Sons: New York, 1995; Chapter 4.
(18) Akoudad, S.; Frère, P.; Mercier, N.; Roncali, J. *J. Org. Chem.* **1999**, *64*, 4267–4272.
(19) Goldoni, F.; Langeveld-Voss, B. M. W.; Meijer, E. W. *Synth. Commun.* **1998**, *28* (12), 2237–2244.
(20) Agarwal, N.; Mishra, S. P.; Kumar, A.; Hung, C.-H.; Ravikanth, M. *Chem. Commun.* **2002**, *22*, 2642–2643.
(21) In the ^{1}H NMR data of ref 18, two triplets (instead of one) are listed. Several errors are found in the ^{13}C NMR peak list: (1) only one thiophenic carbon peak is listed, (2) the 97.2 ppm peak (cannot be assigned either to any thiophenic carbon or the aliphatic side chain) is obviously due to impurity, and (3) a few other peaks in the list (147.6, 71.5, 25.7 ppm) also belong to impurities.
(22) Greeham, N. C.; Moratti, S. C.; Bradley, D. D. C.; Friend, R. H.; Holmes, A. B. *Nature (London)* **1993**, *365*, 628–630.
(23) Samperi, F.; Puglisi, C.; Ferreri, T.; Messina, R.; Cicala, G.; Recca, A.; Restuccia, C. L.; Scamporrino, A. *Polym. Degrad. Stab.* **2007**, *92*, 1304–1315.
(24) Brassett, A. J.; Colaneri, N. F.; Bradley, D. D. C.; Lawrence, R. A.; Friend, R. H.; Murata, H.; Tokito, S.; Tsutsui, T.; Saito, S. *Phys. Rev. B* **1990**, *41*, 10586.
(25) Cornil, J.; dos Santos, D. A.; Beljonne, D.; Bredas, J. L. *J. Phys. Chem.* **1995**, *99*, 5604–5611.
(26) Chen, S.-A.; Chang, E.-C. *Macromolecules* **1998**, *31*, 4899–4907, and references therein.
(27) Yang, S.; Olishevski, P.; Kertesz, M. *Synth. Met.* **2004**, *141*, 171.
(28) *Computational Chemistry: A Practical Guide for Applying Techniques to Real World Problems*, 1st ed.; Young, D. C., Ed.; Wiley-Interscience: New York, 2000.
(29) www.gaussian.com.
(30) Ruedenberg, K.; Scherr, C. W. *J. Chem. Phys.* **1953**, *21*, 1565.

MA802621B